Available online at www.sciencedirect.com
SCIENCE DIRECT®
Journal of Catalysis 221 (2004) 225–233
JOURNAL OF CATALYSIS
www.elsevier.com/locate/jcat

Selective oxidation of *n*-butane in the presence of vanadyl pyrophosphates synthesized by intercalation–exfoliation–reduction of layered $VOPO_4 \cdot 2H_2O$ in 2-butanol

Norihito Hiyoshi,[a] Naoki Yamamoto,[a] Naonori Ryumon,[a] Yuichi Kamiya,[b] and Toshio Okuhara [a,*]

[a] *Graduate School of Environmental Earth Science, Hokkaido University, Sapporo 060-0810, Japan*
[b] *Japan Science and Technology Corporation, 4-1-8 Honcho, Kawaguchi 332-0012, Japan*

Received 19 May 2003; revised 22 July 2003; accepted 1 August 2003

Abstract

Several vanadyl pyrophosphates ($(VO)_2P_2O_7$) with a different microcrystallite structure have been synthesized by a unique process involving the intercalation, exfoliation, and reduction of $VOPO_4 \cdot 2H_2O$. Stepwise thermal treatment of a suspension of $VOPO_4 \cdot 2H_2O$ crystallites in 2-butanol caused the subsequent processes (intercalation, exfoliation, and reduction) to form $VOHPO_4 \cdot 0.5H_2O$ phases. The resulting $VOHPO_4 \cdot 0.5H_2O$ phases were approximately 1–2 μm in lengths and roughly 0.1 μm in thickness with leaf-like shapes. The catalyst derived from the present novel processes was found to be more active and selective (78% selectivity at about 60% conversion at 663 K) than well-known rose-like crystallites (∼1 μm) by the "organic solvent method" using *iso*-butanol and benzyl alcohol. The higher activity of the novel catalyst is attributed to the high surface area (approximately 30 $m^2\ g^{-1}$ after the reaction for 200 h), and the higher selectivity is probably attributable to the pure phase of $(VO)_2P_2O_7$ because of the smaller dimensions of the crystallites and the preferential exposure of the basal plane of $(VO)_2P_2O_7$ due to the leaf shape.

Keywords: Oxidation of *n*-butane; Vanadyl pyrophosphate; Exfoliation; Layered $VOPO_4 \cdot 2H_2O$

1. Introduction

The selective oxidation of *n*-butane to maleic anhydride (MA), which has been carried out commercially using vanadyl pyrophosphate ($(VO)_2P_2O_7$) as a catalyst [1], is limited to about 50% yield, and therefore improvement of the process is highly desirable. To date, various factors that influence the activity and selectivity of the catalyst have been described [2–4], including microstructures of the $(VO)_2P_2O_7$ crystallites, defect sites of the surface, surface compositions (P/V ratio), and oxidation states. Among these factors, the effects of the microstructure are most relevant in the preparation of the catalyst. Studies by Okuhara et al. [2], which demonstrated that the (100) plane of the $(VO)_2P_2O_7$ crystallites is highly selective, whereas the side planes are nonselective, are consistent with reports by Bordes [3], Grasselli and co-workers [4], and Centi et al. [1].

Recently, Koyano et al. [5] claimed that the redox processes of the $(VO)_2P_2O_7$ phase and the oxidized X1 phase, which shows a similar XRD pattern [6] and Raman spectrum [7] to δ-$VOPO_4$, on the surface layers of the basal plane are closely related, in terms of the selective oxidation of *n*-butane; it is important to note that the X1 phase possesses a structure similar to that of $(VO)_2P_2O_7$ [5]. On the other hand, it was also shown that the side planes of $(VO)_2P_2O_7$ were transformed during the reaction to the nonselective β-$VOPO_4$ phase [5]. This anisotropic transformation is in accordance with the structure-sensitive behavior of $(VO)_2P_2O_7$ in its selectivity. Overall, these findings have

* Corresponding author.
E-mail address: oku@ees.hokudai.ac.jp (T. Okuhara).

0021-9517/$ – see front matter
doi:10.1016/j.jcat.2003.08.001

directed us to study the control of the microstructures of the $(VO)_2P_2O_7$ crystallites.

Syntheses of the precursor ($VOHPO_4 \cdot 0.5H_2O$) and the catalyst ($(VO)_2P_2O_7$) have been previously described [8–10]. One such preparation of the precursor is described as the "organic solvent method," and resulted in crystallites with a rose-petal morphology [1,8], which were subsequently used to prepare catalysts that possessed high surface areas and exhibited high activities with moderate selectivities [1,8]. Another preparation method involved the reduction of layered $VOPO_4 \cdot 2H_2O$ using various alcohols [11–15], in which the morphology of the resulting $VOHPO_4 \cdot 0.5H_2O$ crystallites depended on the type of alcohol [11–15].

A unique method to form delaminated sheets of layered materials has attracted much attention, and from the viewpoint of constructing nanostructured materials, this process showed great promise to improve the preparation of our catalyst. To date, using this method, layered materials, including clays [16], chalcogenides [17], titanic acid [18], niobic acid [19], and zirconium phosphate [20], have been exfoliated in aqueous solutions. It is well known that $VOPO_4 \cdot 2H_2O$ possesses a layered structure with high capabilities for intercalation of various molecules [21], and consequently Okuhara and co-workers [22,23] reported on the exfoliation of the intercalation compounds of $VOPO_4 \cdot 2H_2O$ with 4-butylaniline in tetrahydrofuran, and with acrylamide in 1-butanol. Recently, Okuhara and co-workers [24] furthermore found the exfoliation of $VOPO_4 \cdot 2H_2O$ in alcohol.

Herein we describe our studies to evaluate the catalytic performance for *n*-butane oxidation using $(VO)_2P_2O_7$ that was obtained by the intercalation–exfoliation–reduction process of $VOPO_4 \cdot 2H_2O$ in 2-butanol. The catalytic data were compared with those of conventional $(VO)_2P_2O_7$ catalysts. As reported previously [25], this novel preparation route resulted in a catalyst that exhibited excellent selectivity for the oxidation of *n*-butane. The results are discussed on the basis of the stationary catalytic data, microstructure, crystalline phase, oxidation state, and defect sites of the surface.

2. Experimental

2.1. Materials

2.1.1. $VOPO_4 \cdot 2H_2O$

Following the method as described in the literature [26], a mixture of V_2O_5 (24 g, Wako Pure Chem. Ind., Ltd.), aqueous 85% H_3PO_4 (223 g, Wako Pure Chem. Ind., Ltd.), and H_2O (577 cm^3) was refluxed for 24 h. The resulting precipitate was separated by filtration, washed with acetone, and dried under ambient atmosphere. This was identified as $VOPO_4 \cdot 2H_2O$ using XRD and IR [22]. SEM measurements showed that the obtained $VOPO_4 \cdot 2H_2O$ consisted of platelet crystallites with lengths of approximately 20 μm [22]. The surface area was about 1 $m^2\,g^{-1}$ after the evacuation at 423 K (anhydrous $VOPO_4$).

2.1.2. $VOHPO_4 \cdot 0.5H_2O$

Details of the exfoliation–reduction process of $VOPO_4 \cdot 2H_2O$ in various alcohols have been previously reported [24]. Following this method, two different samples were prepared using 2-butanol. Preparation conditions are summarized in Table 1. For the first sample, a mixture of $VOPO_4 \cdot 2H_2O$ (2.0 g) and 2-butanol (50 cm^3, Wako Pure Chem. Ind., Ltd.) was heated stepwise with stirring at 303, 323, 343, and 363 K (1 h at each temperature) to yield a homogeneous yellow solution as the results of intercalation and exfoliation [24]. The homogeneous 2-butanol solution was refluxed for 24 h to form light blue precipitates (reduction) [24], which were separated by centrifugation, washed with acetone, and dried at room temperature. The obtained solid, denoted as EP(2-Bu), was assigned as the precursor $VOHPO_4 \cdot 0.5H_2O$ by XRD and IR, as described below. For the second sample, a mixture of $VOPO_4 \cdot 2H_2O$ (1.0 g) and 2-butanol (50 cm^3) was subjected to the same procedures; however, in this case, precipitates were not formed following the reflux step. By adding a small amount (5 mg) of EP(2-Bu) as seed to the homogeneous solution at the reflux step, precipitates were obtained and were confirmed as $VOHPO_4 \cdot 0.5H_2O$. This sample was denoted as EP(2-Bu)s.

The other series of $VOHPO_4 \cdot 0.5H_2O$ were prepared by the direct reduction of $VOPO_4 \cdot 2H_2O$ with 2-butanol. Two different samples of $VOHPO_4 \cdot 0.5H_2O$ were prepared by

Table 1
Parameters for preparation of precursors

Precursor	Preparation method	Amount of raw materials		Reduction conditions	Others
		$VOPO_4 \cdot 2H_2O$ (g)	2-Butanol (cm^3)		
EP(2-Bu)s	Exfoliation[a]	1.0	50	378 K, 24 h	Addition of seed[c]
EP(2-Bu)	Exfoliation[a]	2.0	50	378 K, 24 h	
P(2-Bu)	Direct reduction[b]	10.0	100	378 K, 18 h	
P(2-Bu)h	Direct reduction[b]	2.5	25	423 K, 15 h	Using autoclave[d]

[a] Prepared by intercalation–exfoliation–reduction process of $VOPO_4 \cdot 2H_2O$ in 2-butanol.
[b] Prepared by direct reduction of $VOPO_4 \cdot 2H_2O$ with 2-butanol.
[c] A small amount (5 mg) of $VOHPO_4 \cdot 0.5H_2O$ (EP(2-Bu)) was added to exfoliated solution.
[d] Prepared by heating in a Teflon vessel equipped with a stainless-steel jacket.

such direct reduction method. For the first sample, a mixture of $VOPO_4 \cdot 2H_2O$ (10 g) and 2-butanol (100 cm^3) was directly refluxed at 378 K for 18 h, resulting in a light blue solid ($VOHPO_4 \cdot 0.5H_2O$), which was denoted as P(2-Bu). The second sample of $VOHPO_4 \cdot 0.5H_2O$, which was denoted as P(2-Bu)h, was prepared by heating a mixture of $VOPO_4 \cdot 2H_2O$ (2.5 g) and 2-butanol (25 cm^3) at 423 K for 15 h in a Teflon vessel (45 cm^3) equipped with a stainless-steel jacket.

Finally, a precursor $VOHPO_4 \cdot 0.5H_2O$, which was denoted as OSM, was prepared following conventional methods as described in the literature [27], through the "organic solvent method" using V_2O_5 (14.6 g), H_3PO_4 (16.2 g, Merck), *iso*-butanol (90 cm^3, Wako Pure Chem. Ind., Ltd.), and benzyl alcohol (60 cm^3, Wako Pure Chem. Ind., Ltd.).

2.2. Characterization

XRD patterns of the solid samples were measured using an XRD diffractometer (Miniflex Rigaku) with Cu-K_α radiation. The surface area was determined by the BET method using an automatic adsorption apparatus (BELSORP 28SA, BEL Japan); the precursors and catalysts were evacuated at 423 and 523 K, respectively. SEM images were taken using S-2100 (Hitachi). Scanning transmission electron microscopy (STEM) images were taken with HD-2000 (Hitachi) operating at 200 kV.

The average oxidation numbers of V in the sample bulk were determined by redox-titration using $KMnO_4$ [28]. X-ray photoelectron spectra (XPS) were obtained with a Shimadzu XPS-7000 with Mg-K_α radiation. All spectra were referenced to the carbon 1s peak at a binding energy of 284.5 eV. $VOPO_4 \cdot 2H_2O$ and $(VO)_2P_2O_7$ were used as standard samples for V^{5+} and V^{4+}, respectively. The standard $(VO)_2P_2O_7$ was prepared in a flow reactor at 663 K by a thermal treatment of EP(2-Bu)s in He flow for 5 h. To avoid an oxidation of the standard $(VO)_2P_2O_7$ with air, the sample was transferred from the reactor to the sample chamber of the XPS apparatus under an atmosphere of N_2. The oxidation number of the surface was estimated in the same manner as that reported [29].

2.3. Catalytic oxidation of *n*-butane

Oxidation of *n*-butane was carried out at 663 K in a flow reactor (Pyrex tube, 10 mm inside diameter) with a mixture of *n*-butane (1.5 vol%), O_2 (17 vol%), and He (balance) under atmospheric pressure. After the precursor (0.7–1.4 g) was placed in the reactor, the reactant gas was introduced at a rate of 20 $cm^3\,min^{-1}$. The temperature was raised to 663 K at a rate of 5 $K\,min^{-1}$, and when the temperature reached 663 K, the gas at the outlet of the reactor was analyzed using on-line gas chromatography. For *n*-butane and MA, an FID GC (Shimadzu GC8A) with a Porapak QS column (1 m) was used. A high-speed GC (Aera M200) with Porapak Q and Molecular Sieves 5A columns was utilized for the analysis of CO, CO_2, and O_2 in the gas phase.

Since the conversion and selectivity gradually changed with time, the data for stationary conversion and selectivity were collected for 200 h of the reaction. After 200 h, the W/F dependence of conversion was determined (W is the catalyst weight and F is the total flow rate) by changing the total flow rate. Catalyst samples that exhibited stationary conversions were denoted as C (e.g., EC(2-Bu) by exfoliation–reduction, and C(2-Bu) by direct reduction).

3. Results

3.1. Microstructures of the precursors and catalysts

Fig. 1 shows the SEM images of the starting $VOPO_4 \cdot 2H_2O$ and the precursors. As described previously [22,23], SEM analysis revealed that $VOPO_4 \cdot 2H_2O$ consisted of platelet particles with lengths of approximately 20 μm (Fig. 1a). However, the microstructures (shape and dimension) of the precursors were quite different from those of starting $VOPO_4 \cdot 2H_2O$, and were significantly sensitive to the preparation method. EP(2-Bu)s (Fig. 1b) and EP(2-Bu) (Fig. 1c), which were obtained through exfoliation, exhibited smaller leaf-like particles with lengths of 1–2 μm, and the length of the crystallites for EP(2-Bu)s was smaller than that for EP(2-Bu). On the other hand, the crystallites of P(2-Bu) (Fig. 1d) and P(2-Bu)h (Fig. 1e), which were prepared by direct reduction, were composed of well-developed platelets having lengths of about 5 and 10 μm, respectively. The OSM

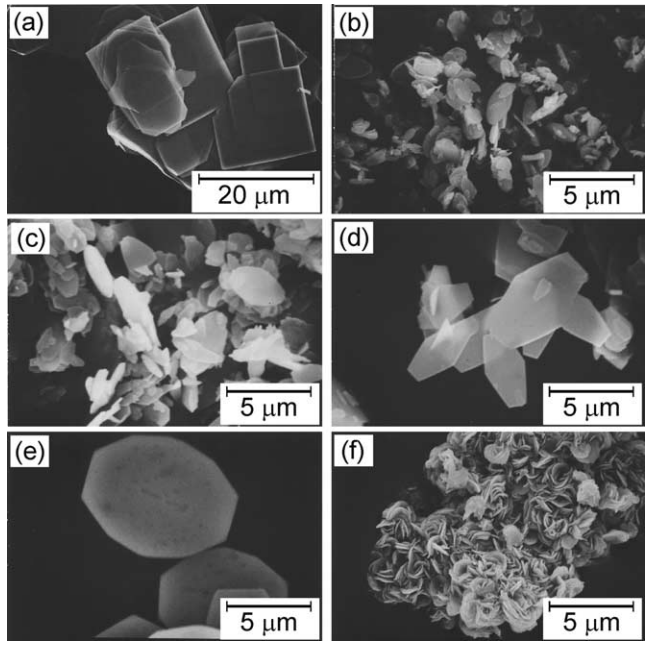

Fig. 1. SEM images of (a) $VOPO_4 \cdot 2H_2O$ and the precursors ($VOHPO_4 \cdot 0.5H_2O$), (b) EP(2-Bu)s, (c) EP(2-Bu), (d) P(2-Bu), (e) P(2-Bu)h, and (f) OSM.

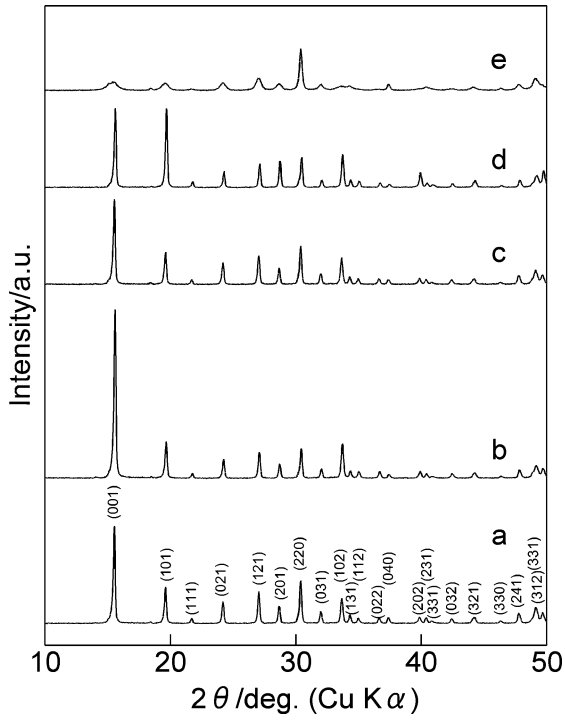

Fig. 2. XRD patterns of the precursors ($VOHPO_4 \cdot 0.5H_2O$) (a) EP(2-Bu)s, (b) EP(2-Bu), (c) P(2-Bu), (d) P(2-Bu)h, and (e) OSM.

Table 2
Properties of the precursors ($VOHPO_4 \cdot 0.5H_2O$)

Precursor	SA[a]	Average length[b]	Thickness[c]	n of V^{n+}	
	($m^2\,g^{-1}$)	(μm)	(nm)	Bulk[d]	Surface[e]
EP(2-Bu)s	7.6	1	110	4.01	4.00
EP(2-Bu)	5.6	2	150	4.04	4.04
P(2-Bu)	3.1	5	250	3.97	4.15
P(2-Bu)h	1.0	10	830	3.98	4.08
OSM[f]	9.1	1	92	3.99	4.31

[a] After pretreatment at 423 K in a vacuum.
[b] Estimated from SEM.
[c] Estimated from the surface area and the length [Eq. (1)].
[d] Average oxidation number of vanadium estimated by redox-titration.
[e] Estimated from XPS.
[f] Prepared by the organic solvent method [27].

precursor consisted of rose-petal particles with lengths of approximately 1 μm, as reported previously [27].

The XRD patterns of the precursors are shown in Fig. 2. All the precursors exhibited patterns attributable to the $VOHPO_4 \cdot 0.5H_2O$ phase, while the relative intensities differed depending on the precursors. The relative intensity of the two main peaks ($I(220)/I(001)$) followed the order: OSM > P(2-Bu) = EP(2-Bu)s = P(2-Bu)h > EP(2-Bu).

The surface area, length and thickness of the particles, and the oxidation number of V of the bulk and surface for the precursors are summarized in Table 2. The values for the thickness were too large to estimate from the line width of the XRD peaks. The values for the length were estimated from the SEM images. The thickness (t) of the particles (or crystallites) was calculated from Eq. (1) using density (D; 2.822 $g\,cm^{-3}$), which was calculated from the lattice constant of $VOHPO_4 \cdot 0.5H_2O$, surface area (S; $m^2\,g^{-1}$), and length of the particles (L; μm), which was estimated from SEM images:

$$2000/t + 4/L = S \times D. \quad (1)$$

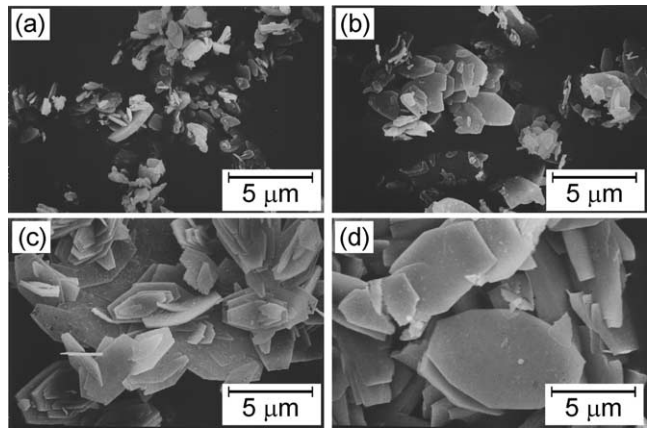

Fig. 3. SEM images of the catalysts (a) EC(2-Bu)s, (b) EC(2-Bu), (c) C(2-Bu), and (d) C(2-Bu)h.

As shown in Table 2, the values for the thickness of the precursors followed in the order: P(2-Bu)h > P(2-Bu) > EP(2-Bu) > EP(2-Bu)s > OSM, in which the maximum differences in the thickness were about 10-fold. The oxidation numbers of V of the bulk for these precursors were approximately 4.0 (Table 2). The surface oxidation numbers for the precursors, except OSM, were in the range of 4.00–4.15, while OSM gave a higher value (4.31) than the other precursors (Table 2).

Fig. 3 presents the SEM images of the catalysts, which were defined as the samples after the reaction for 200 h and gave the stationary activity and selectivity. The morphologies of each catalyst were consistent with those of the corresponding precursor. Similarly, the SEM micrograph of OSM resembled that of its precursor (data not shown).

The XRD patterns of the catalysts after the reaction for 200 h are shown in Fig. 4. Both EC(2-Bu)s and EC(2-Bu) showed the patterns of the $(VO)_2P_2O_7$ phase [30]. The peaks were relatively broad in comparison with those of the corresponding precursors (Figs. 2a and b) and the relative intensity of the (200) peak for EC(2-Bu) was stronger than that for EC(2-Bu)s. It is considered that $VOHPO_4 \cdot 0.5H_2O$ transforms to $(VO)_2P_2O_7$ topotactically. The difference in the relative intensity of the XRD peaks would reflect the difference in the morphology of the corresponding precursors. As shown in Fig. 4e, OSM was also identified as the $(VO)_2P_2O_7$ phase. However, it is important to note that the peaks due to α_{II}-$VOPO_4$ [31] and δ-$VOPO_4$ [31] were detected for C(2-Bu) and C(2-Bu)h besides that of $(VO)_2P_2O_7$, being that α_{II}-$VOPO_4$ was the main phase for the latter.

Table 3 summarizes the surface area, length and thickness of the particle, and the oxidation numbers of V of the bulk and surface for the catalysts, as well as values for the activ-

Table 3
Physical and catalytic properties of the catalysts

Catalyst	SA[a]	Length[b]	Thickness[c] (nm)		$F(100)$[d]	n of V^{n+}		Activity[g]	Selectivity[h]
	($m^2\,g^{-1}$)	(μm)	SA	XRD		Bulk[e]	Surface[f]	(10^{-4} mol $g^{-1}\,h^{-1}$)	(%)
EC(2-Bu)s	28	1	23	13	0.96	4.08	4.23	17 (0.58)	77.5 (50.9)
EC(2-Bu)	23	2	27	22	0.97	4.14	4.38	14 (0.60)	77.1 (49.5)
C(2-Bu)	14	5	44	–[i]	0.98	4.38	4.39	9 (0.62)	75.0 (48.1)
C(2-Bu)h	10	10	61	–[i]	0.99	4.55	4.23	4 (0.45)	71.7 (43.2)
OSM[j]	23	1	27	13	0.95	4.07	4.31	13 (0.55)	72.6 (46.0)
C(2-Bu)h-He	11	10	57	14	0.99	3.99	4.31	5 (0.48)	71.8 (42.8)

[a] After pretreatment at 523 K in a vacuum.
[b] Estimated from SEM.
[c] SA, estimated from surface area and the length [Eq. (1)], and XRD, estimated from the linewidth of the diffraction peak of the (100) plane.
[d] Fraction of area of the (100) plane estimated from length and thickness from the surface area.
[e] Average oxidation number of vanadium estimated by redox-titration.
[f] Estimated from XPS.
[g] Values in the parentheses are the specific activity per surface area (10^{-4} mol $m^{-2}\,h^{-1}$).
[h] Values in the parentheses are the conversion at which the selectivity was measured.
[i] Mixed phases of $(VO)_2P_2O_7$ and α_{II}-$VOPO_4$.
[j] Prepared by the organic solvent method [27].

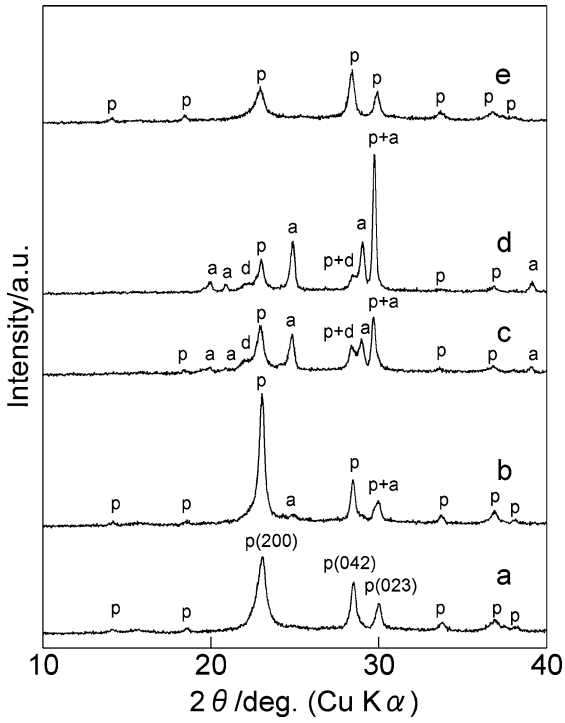

Fig. 4. XRD patterns of the catalysts (a) EC(2-Bu)s, (b) EC(2-Bu), (c) C(2-Bu), (d) C(2-Bu)h, and (e) OSM. Marks of p, a, and d show $(VO)_2P_2O_7$ and α_{II}-$VOPO_4$ and δ-$VOPO_4$, respectively. These data were taken at 200 h of the reaction.

ity and selectivity, in which the catalytic data were collected after the stationary state at 663 K. The thicknesses were estimated from the surface area [Eq. (1)] using the density of $(VO)_2P_2O_7$ (3.342 g cm^{-3}) or XRD; values for the thickness of the crystallites using XRD varied from identical to about one-fifth those of the precursors (Table 3). The oxidation numbers of V of the catalyst bulk for C(2-Bu) and C(2-Bu)h greatly exceeded 4.0, while those for EC(2-Bu)s and EC(2-Bu) were close to 4.0, consistent with the XRD. It should be emphasized that these catalysts gave approximately the same oxidation number of the surface. This inhomogeneity of the oxidation state of V between the bulk and the surface will be discussed in further detail below.

The fraction of the surface area of the (100) plane (denoted as $F(100)$ in Table 3) to the total surface area was estimated from the length, thickness (from the surface area), and total surface area. It was observed that the values of $F(100)$ were higher than 0.95 for all the catalysts, and that the differences between the values of the fraction were small among these catalysts.

Fig. 5 presents the phase contrast STEM images of the precursors (EP(2-Bu)s and P(2-Bu)h) and catalysts (EC(2-Bu)s and C(2-Bu)h), and the SEM images taken on the same particles. The lengths of the precursors and catalysts estimated from STEM images were consistent with those from the SEM images (Figs. 1 and 3). No distinct contrast in the particles (in STEM images) was observed for both the precursors, suggesting that the particles of these precursors consisted of single crystals. On the contrary, mosaic patterns consisting of the microcrystallites (ca. 50 nm) were observed inside the particles of the catalysts (Figs. 5c and d). In the case of C(2-Bu)h (Fig. 5d), two kinds of the microcrystallites showing the contrasts of dark and light gray existed, while the particle of EC(2-Bu)s was made up by the oblong microcrystallites having a uniform dark contrast. In addition, the distinct shell being dark contrast along the periphery of the particle was observed for both catalysts.

3.2. Selective oxidation of n-butane

Fig. 6 shows the W/F dependence of the conversion for n-butane oxidation at 663 K, where W is the weight of the catalyst (kg) and F is the flow rate of n-butane (mol h^{-1}). The catalytic activities were estimated from the initial slopes of these curves. Among the catalysts, EC(2-Bu)s was found

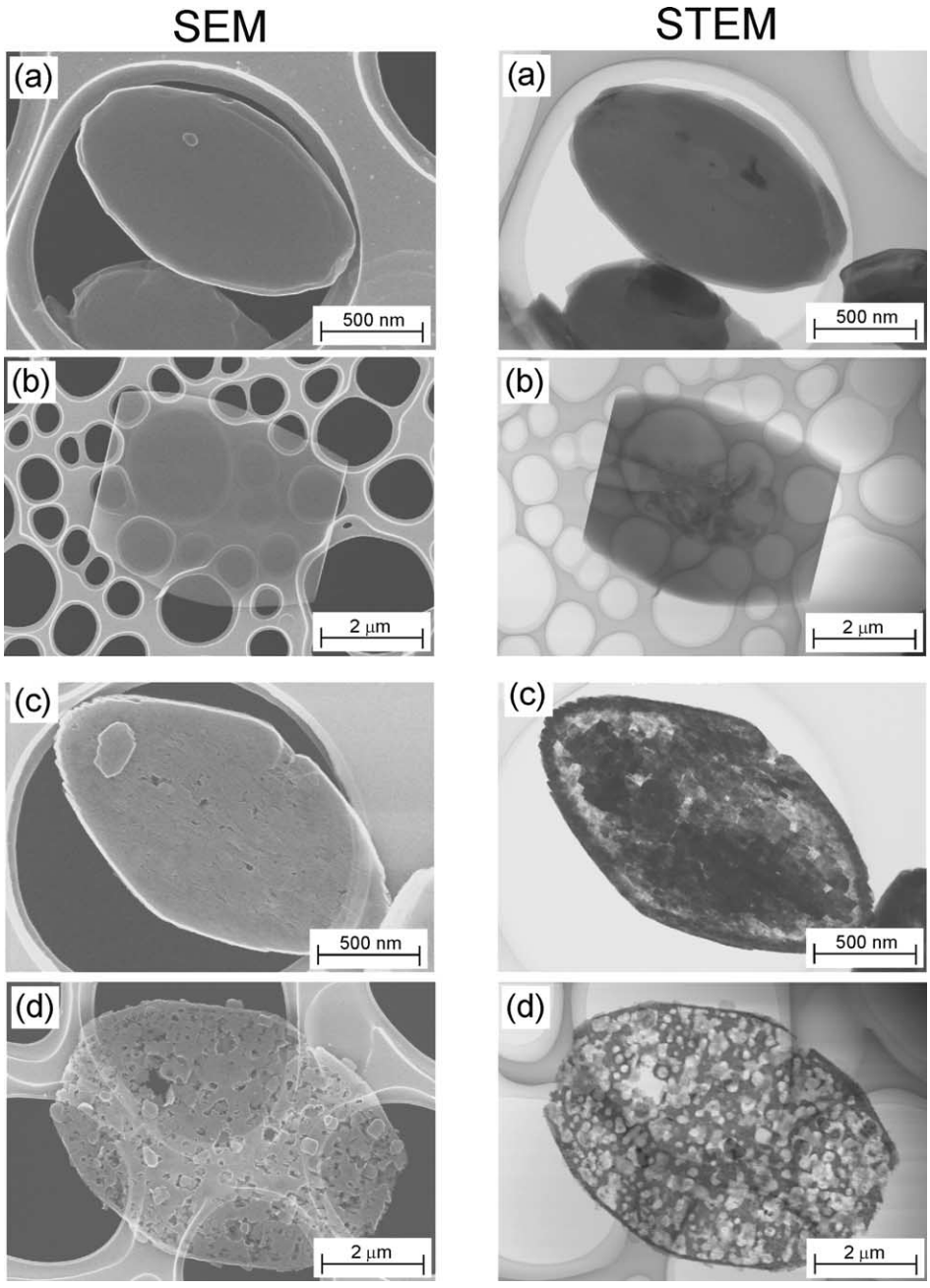

Fig. 5. STEM images of the precursors and catalysts (a) EP(2-Bu)s, (b) P(2-Bu)h, (c) EC(2-Bu)s, and (d) C(2-Bu)h. Pictures in the left and right hands are SEM and STEM images, respectively.

to be the most active, and the activities were in the following order: EC(2-Bu)s > EC(2-Bu) > OSM > C(2-Bu) > C(2-Bu)h; the order is consistent with that of the surface areas (Table 3), as described below.

As shown in Fig. 7, the selectivity to MA (on the basis of *n*-butane) is plotted against the conversion of *n*-butane. It should be noted that the selectivities of EC(2-Bu) and EC(2-Bu)s were higher than that of conventional OSM, as well as those of C(2-Bu) and C(2-Bu)h. Furthermore, it should be emphasized that the selectivity for EC(2-Bu)s reached about 78% at low conversion levels, and was retained at 75% at the 80% conversion level (Fig. 7).

4. Discussion

$(VO)_2P_2O_7$ is the active component of the commercial catalyst for the selective oxidation of *n*-butane [1]. Since the transformation of the precursor ($VOHPO_4 \cdot 0.5H_2O$) to $(VO)_2P_2O_7$ is topotactic [11], that is, the dehydration takes place retaining its microstructure, control of the microstructure of the precursor is indispensable in obtaining the desirable crystallites of $(VO)_2P_2O_7$ catalyst, and therefore a novel method to prepare the catalyst crystallites with a suitable microstructure is highly desirable.

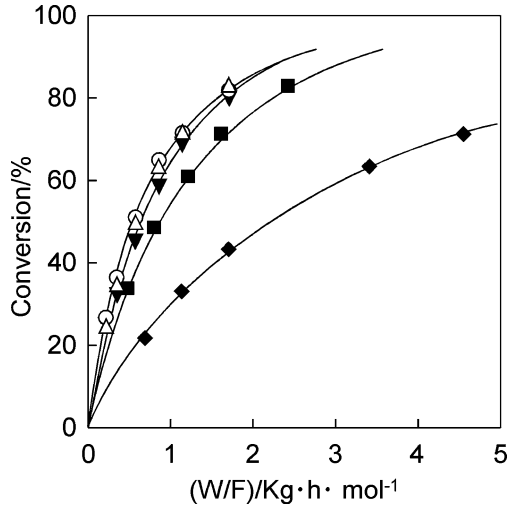

Fig. 6. W/F dependence of conversion of n-butane: (○) EC(2-Bu)s, (△) EC(2-Bu), (■) C(2-Bu), (◆) C(2-Bu)h, and (▼) OSM. The reaction was performed at 663 K with the mixture of n-butane 1.5%, O_2 17%, and He (balance). The data were collected at 200 h of the reaction.

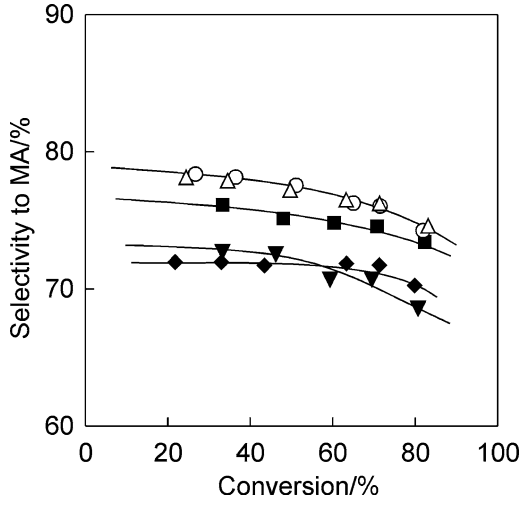

Fig. 7. Changes of selectivity to maleic anhydride as a function of conversion of n-butane: (○) EC(2-Bu)s, (△) EC(2-Bu), (■) C(2-Bu), (◆) C(2-Bu)h, and (▼) OSM. The reaction was performed at 663 K with the mixture of n-butane 1.5%, O_2 17%, and He (balance). The data were collected at 200 h of the reaction.

It is accepted that the selectivity toward MA depends on the type of the crystal plane of $(VO)_2P_2O_7$ crystallites [2–4]. Okuhara et al. [2] have concluded, on the basis of experimental results, that the basal (100) plane is selective, whereas the side planes are nonselective. A sample of $(VO)_2P_2O_7$ consisting of platelet crystallites ($\sim$5 μm), which was prepared from the reduction of $VOPO_4 \cdot 2H_2O$, exhibited about 60% selectivity. When covered with SiO_2 overlayers by the CVD method, this $(VO)_2P_2O_7$ catalyst sample became inactive. By fracturing the SiO_2-covered $(VO)_2P_2O_7$, side planes were newly created, and as a result, the fractured sample was nonselective; this indicated that the selective plane of the crystallites is the basal plane, on which the $V^{4+}(=O)$–O–V^{4+} pair sites are present. Furthermore, Koyano et al. [5] found that the oxidation of the basal plane resulted in the X1 phase (V^{5+}), which resembles $(VO)_2P_2O_7$, but the side planes are oxidized to the nonselective β-$VOPO_4$ phase. These findings are in good agreement with the anisotropic sensitivity for the oxidation of n-butane, as discussed above.

In addition to the effects of the microstructure, the effects of the distortion of the crystallites have also been indicated. Trifirò and co-workers [8] and Hattori and co-workers [32] have suggested that the high catalytic performance of $(VO)_2P_2O_7$ prepared by the organic solvent method and thus consisting of rose-petal shapes is due to the distortion of the basal plane. Gai and Kourtakis [33] have claimed that V^{3+} species associated with defect sites play an important role in the selective oxidation of n-butane. Volta and co-workers [7] have stressed the important role of V^{5+} species within the $(VO)_2P_2O_7$ phase, and have concluded that the dispersed V^{5+} species were critical for the formation of MA, whereas excess surface V^{5+} species was detrimental to the selectivity toward MA.

In the present study, attempts were undertaken to prepare $(VO)_2P_2O_7$ crystallites having the shape of thin layers in order to expand the fraction of the basal plane by the delamination of layered $VOPO_4 \cdot 2H_2O$ through the exfoliation process. It has been reported that the exfoliations of clays [16], chalcogenides [17], titanic acid [18], niobic acid [19], and zirconium phosphate [20] were carried out in aqueous solutions. We have already demonstrated the exfoliation of $VOPO_4 \cdot 2H_2O$ through the formation of intercalation compounds with 4-butylaniline or acrylamide [22,23]. This process provided for the preparation of highly active SiO_2-supported catalysts exhibiting a selectivity of 54% [34]. More recently, we have found that $VOPO_4 \cdot 2H_2O$ can be exfoliated in various alcohols to form delaminated sheets of $VOPO_4$ [24].

We wish to emphasize that the $(VO)_2P_2O_7$ crystallites obtained in these studies by the novel "exfoliation–reduction" method were highly active and selective for the n-butane oxidation. Table 3 and Figs. 6 and 7 clearly demonstrate the improved catalytic performances of catalyst EC(2-Bu)s; since its specific activity (per surface area) was nearly equal to other catalysts, the high activity of this "exfoliation" catalyst is attributable to the higher surface area (Table 3). It is reasonable to suggest that the "exfoliation process" increased the surface area of the final catalyst. In terms of selectivity, it was remarkable that these "exfoliated" catalysts, EC(2-Bu)s and EC(2-Bu), exhibited improved selectivities as compared to other conventional catalysts. The selectivities of these exfoliated catalysts exceeded 77% at about 50% conversion (Table 3).

The influence of the fraction of the basal plane should be taken into consideration. However, as shown in Table 3, for all catalysts, the fractions of the basal plane were over 0.95. Therefore, the differences in the selectivity cannot be directly attributed to the fraction of the basal plane, while the preferential exposure of the basal plane

is a necessary condition. Subsequently, as another factor that can influence the selectivity, which was disclosed in the present study, the presence of oxidized phases such as α_{II}-$VOPO_4$ and δ-$VOPO_4$ in some catalysts was considered. As shown in Fig. 4, the platelet-like catalysts, C(2-Bu) and C(2-Bu)h, consisted of $(VO)_2P_2O_7$, α_{II}-$VOPO_4$, and δ-$VOPO_4$ phases. A previous report [31] showed that α_{II}-$VOPO_4$ yielded only 20–30% selectivity toward MA, whereas $(VO)_2P_2O_7$ yielded about 70% selectivity. Surprisingly, although the main phase of C(2-Bu)h was α_{II}-$VOPO_4$, and not $(VO)_2P_2O_7$, C(2-Bu)h showed a moderate selectivity to MA ($\sim$70%).

As shown in Table 3, the oxidation number of V of the bulk for the exfoliation catalysts (EC(2-Bu)s and EC(2-Bu)) was nearly 4.0, while those for C(2-Bu) and C(2-Bu)h significantly exceeded 4.0 (Table 3). On the contrary, the surface oxidation state scarcely differed among these catalysts, being about $V^{4.2+}$. The exfoliated catalysts gave the XRD pattern of $(VO)_2P_2O_7$ (Fig. 4), consistent with its oxidation number of V of the catalyst bulk (Table 3). These results indicate that C(2-Bu) and C(2-Bu)h contained the oxidized phases such as α_{II}-$VOPO_4$ and δ-$VOPO_4$ inside of the catalyst particles. The STEM images of C(2-Bu)h demonstrated the inhomogeneity of the particle between the surface and the bulk for C(2-Bu)h (Fig. 5d). The selective oxidation of *n*-butane over $(VO)_2P_2O_7$ has been accepted to proceed via a redox mechanism involving V^{4+} and V^{5+} at a few surface layers [1,5], thus, the surface layers after the steady-state reaction would contain the V^{5+} phase to some extent [5]. Hutchings et al. [35] proposed that the active center for *n*-butane activation and MA formation comprises a V^{4+}/V^{5+} couple that is well dispersed on the catalyst surface, although the exact nature of the active sites is still a matter of debate. In the present study, the catalyst surfaces of both the exfoliated and the conventional catalysts were actually little oxidized, which is consistent with the above idea, and it is worthy of note that the oxidized level of the surface was the same among these catalysts (Table 3). This shows that the surface layers of the conventional catalysts were similar to those for the exfoliation ones. That is the reason for the moderately high selectivity ($\sim$70%) of C(2-Bu)h, despite the main phase of α_{II}-$VOPO_4$.

Kiely et al. [36] pointed out that, when the large crystallites of $VOHPO_4 \cdot 0.5H_2O$ were activated in the reactant mixture, dehydration to $(VO)_2P_2O_7$ proceeded preferentially at the periphery of the crystallites at the initial stages, and in contrast, $VOHPO_4 \cdot 0.5H_2O$ in the bulk of the crystallites tended to transform to α_{II}-$VOPO_4$. Our present results are consistent with the findings of Kiely et al. and further revealed that as the length and thickness of $VOHPO_4 \cdot 0.5H_2O$ crystallites decreased, the oxidation of $VOHPO_4 \cdot 0.5H_2O$ to α_{II}-$VOPO_4$ was greatly suppressed during the activation process. Therefore, the differences in the selectivity in Table 3 can be explained as the difference sizes of the catalyst crystallites. The small leaf-like microcrystallites of the precursor can be prepared using the exfoliation method, and a pure $(VO)_2P_2O_7$ phase is subsequently formed from these precursors. The pure $(VO)_2P_2O_7$ is one of reason for the high selectivity for the exfoliation catalysts.

It is important to consider that the selectivity of the basal plane should be different depending on the type of the crystallites. It is reasonable to suggest that the nature and amount of the defects on the basal plane are different among these crystallites. We have examined the influence of the α_{II}-$VOPO_4$ phase that occurs in the inside of the crystallites of C(2-Bu)h. To avoid the formation of the V^{5+} phase, precursor P(2-Bu)h was dehydrated in He instead of the reactant mixture, and the resulting sample, C(2-Bu)h-He, was shown to have a surface area of 10 $m^2\,g^{-1}$ with a crystallite shape similar to that of C(2-Bu)h (Table 3). The oxidation number of V of the catalyst bulk was determined to be 3.99, which was as expected. In addition, the surface oxidation state of EC(2-Bu)h-He was the same as that of C(2-Bu)h. Accordingly, XRD studies have revealed that C(2-Bu)h-He contains a pure phase of $(VO)_2P_2O_7$. The catalytic activity of C(2-Bu)h-He was slightly higher than that of C(2-Bu)h (Table 3), and correspondingly, its selectivity was similar to that of C(2-Bu)-h at 663 K. These results indicated that the influence of α_{II}-$VOPO_4$ that is located within the crystallites on the catalytic property was not so large, and therefore, the essential functions of these catalysts are governed by the structure of the surface layers, which is consistent with the conclusion by Koyano et al. [5]. Recently Duvauchelle and Bordes [37] inferred that a mosaic texture was formed during the dehydration process of $VOHPO_4 \cdot 0.5H_2O$ to $(VO)_2P_2O_7$ and presumed that the intercrystallite boundaries played an important role in the selective oxidation of *n*-butane. The influences of the microstructure of the catalyst crystallites on the activity and selectivity must be critical, and these are issues to be solved in the future.

5. Conclusion

The present study demonstrates that $(VO)_2P_2O_7$ catalysts prepared by a novel exfoliation method were highly active and selective for selective oxidation of *n*-butane as compared with the conventional catalysts obtained by direct reduction or the organic solvent method. These new catalysts consisted of crystallites like small leaves and have a pure $(VO)_2P_2O_7$ structure in bulk after the activation in the reactant mixture. The absence of the oxidized crystalline phases such as α_{II}-$VOPO_4$ and δ-$VOPO_4$ as well as highly dispersed V^{5+} species on the surface is responsible for the high selectivity to MA.

Acknowledgment

This work was partly supported by New Energy and Industrial Technology Development Organization (NEDO).

References

[1] G. Centi, F. Trifirò, J.R. Ebner, V.M. Franchetti, Chem. Rev. 88 (1988) 55.
[2] T. Okuhara, K. Inumaru, M. Misono, Chem. Lett. (1992) 1955; T. Okuhara, K. Inumaru, M. Misono, in: S.T. Oyama, J.W. Hightower (Eds.), Catalytic Selective Oxidation, in: ACS Symposium Series, Vol. 523, Am. Chem. Society, Washington, DC, 1993, p. 156.
[3] E. Bordes, Catal. Today 16 (1993) 27.
[4] P.A. Agaskar, L. DeCaul, R.K. Grasselli, Catal. Lett. 23 (1994) 339.
[5] G. Koyano, T. Okuhara, M. Misono, J. Am. Chem. Soc. 120 (1998) 767.
[6] E. Bordes, P. Courtin, J. Chem. Soc., Chem. Commun. (1985) 294.
[7] F.B. Abdelcuahab, R. Olier, N. Guilhanme, F. Lefebvre, J.C. Volta, J. Catal. 134 (1992) 151.
[8] G. Busca, F. Cavani, G. Centi, F. Trifirò, J. Catal. 99 (1986) 400.
[9] B.K. Hodnett, Catal. Rev.-Sci. Eng. 27 (1985) 373.
[10] G. Cavani, F. Trifirò, Stud. Surf. Sci. Catal. 91 (1995) 1.
[11] J.W. Johnson, D.C. Johnston, A.J. Jacobson, J.F. Brody, J. Am. Chem. Soc. 106 (1984) 8123.
[12] I.J. Ellison, G.J. Hutchings, M.T. Sananes, J.C. Volta, J. Chem. Soc., Chem. Commun. (1994) 1093.
[13] G.J. Hutching, M.T. Sananes, S. Sajip, C.J. Kiely, A. Burrows, I.J. Ellison, J.C. Volta, Catal. Today 33 (1997) 161.
[14] M.T. Sananes, I.J. Ellison, S. Sajip, A. Burrows, C.T. Kiely, J.C. Volta, G.J. Hutching, J. Chem. Soc., Faraday Trans. 92 (1996) 137.
[15] J.K. Bartley, I.J. Ellison, A. Delimitis, C.J. Kiely, A.Z. Isfahani, C. Rhodes, G.J. Hutching, Phys. Chem. Chem. Phys. 3 (2001) 4606.
[16] E.R. Kleinfeld, G.S. Furgson, Science 265 (1994) 370.
[17] P. Joensen, R.F. Frndt, S.R. Morris, Matter. Res. Bull. 21 (1986) 457.
[18] T. Sasaki, S. Nakano, S. Yamauchi, M. Watanabe, Chem. Mater. 9 (1997) 602.
[19] R. Abe, K. Shinohara, A. Tanaka, M. Hara, J.N. Kondo, K. Domen, Chem. Mater. 9 (1997) 2179.
[20] S.W. Keller, H.-N. Kim, T.E. Mallouk, J. Am. Chem. Soc. 116 (1994) 8817.
[21] L. Benes, K. Melanova, V. Zima, J. Kalousova, J. Votinsky, Inorg. Chem. 36 (1997) 2850.
[22] T. Nakato, Y. Furumi, N. Terao, T. Okuhara, J. Mater. Chem. 10 (2000) 737.
[23] N. Yamamoto, T. Okuhara, T. Nakato, J. Mater. Chem. 11 (2001) 1858.
[24] N. Yamamoto, N. Hiyoshi, T. Okuhara, Chem. Mater. 14 (2002) 3882.
[25] N. Hiyoshi, Y. Yamamoto, T. Okuhara, Chem. Lett. (2001) 484.
[26] G. Ladwig, Z. Anorg. Allg. Chem. 338 (1965) 266.
[27] H. Igarashi, K. Tsuji, T. Okuhara, M. Misono, J. Phys. Chem. 97 (1993) 7065.
[28] B.K. Hodnett, P. Permanne, B. Delmen, Appl. Catal. 6 (1983) 231.
[29] M. Abon, K.E. Bere, A. Tuel, P. Delochere, J. Catal. 156 (1995) 28.
[30] Y.E. Gorbunova, S.E. Linde, Dokl. Akad. Nauk SSSR 245 (1979) 584.
[31] T. Shimoda, T. Okuhara, M. Misono, Bull. Chem. Soc. Jpn. 58 (1985) 2163.
[32] A. Satsuma, Y. Tanaka, T. Hattori, Y. Murakami, Appl. Surf. Sci. 121/122 (1997) 496.
[33] P.L. Gai, K. Kourtakis, Science 267 (1995) 661.
[34] N. Hiyoshi, N. Yamamoto, N. Terao, T. Nakato, T. Okuhara, Stud. Surf. Sci. Catal. 130 (2000) 1715.
[35] G.J. Hutchings, C.J. Kiely, M.T. Sananes-Schulz, A. Burrows, J.C. Volta, Catal. Today 40 (1998) 273.
[36] C.J. Kiely, A. Burrows, G.J. Hutchings, K.E. Bere, J.C. Volta, A. Tuel, M. Abon, Faraday Discuss. 105 (1996) 103.
[37] N. Duvauchelle, E. Bordes, Catal. Lett. 57 (1999) 81.